Advanced Materials Research Vol 1117 (2015) pp 107-113
© (2015) Trans Tech Publications, Switzerland
doi:10.4028/www.scientific.net/AMR.1117.107

Submitted: 2014-10-30
Revised: 2015-02-28
Accepted: 2015-03-12

Materials and photosensor devices with high radiation stability

Ilariy Rarenko[1], Dmytro Korbutyak[2], Volodymyr Koshkin[3], Borys Danilchenko[4], Leonid Kosyachenko[1], Petro Fochuk[1], Valeriy Sklyarchuk[1], Zinaida Zakharuk[1], Sergey Dremlyuzhenko[1], Anna Rarenko [1], Yevgeniy Nikonyuk[1], Vasyl Klad'ko[2], Lubomyr Demchyna[2], Sergiy Budzulyak[2], Nadiya Vakhnyak[2], Arturs Medvid'[5*], Edvins Dauksta[5]

[1]Chernivtsy National University, Kotsyubinsky str. 2, Chernivtsy, 58012, Ukraine

[2]V.E. Lashkaryov Institute of Semiconductor Physics NAS of Ukraine, 41, Nauky ave., Kiev, Ukraine

[3]Kharkiv Polytechnic University, Kharkiv, Ukraine

[4]Institute of Physics of NASU, Kiev, Ukraine

[5]Riga Technical University, Paula Valdena str. 7, Riga, Latvia

e-mail: medvids@latnet.lv

Keywords: photosensor, γ-radiation, radiation stability

Introduction. Semiconductor $Hg_3In_2Te_6$ crystals and their analogous are solid solutions of In_2Te_3 and HgTe. $Hg_3In_2Te_6$ crystals are congruently melted as chemical compound. Like In_2Te_3 the $Hg_3In_2Te_6$ crystal has cubic crystal lattice with stoichiometric vacancies in their crystal structure. The electroconductivity, photoconductivity, mechanical, chemical properties of the crystals do not deteriorate after their irradiation by γ-photons with energies up to 1 MeV and doses up to 10^{18} cm^{-2}, by electrons with energies up to 300 MeV and doses up to 10^{19} cm^{-2} and by mixed reactor irradiation (filtered slow neutrons) with doses up to 10^{19} cm^{-2} [1,2]. This feature is determined by high concentration (~10^{21} cm^{-3}) of stoihiometric vacancies (V_s) in crystal structure, where every third In-cation node is empty. These V_s are electroneutral, they capture all impurity atoms in these crystals and kept them in electroneutral state too. On the other hand, this feature does not allow forming direct p-n junctions in these crystals by introducing the impurities. However, we have developed p-n junction analogues in form of Schottky diodes and corresponding photodiodes with semitransparent metal layer on single crystal $Hg_3In_2Te_6$ substrate that allows irradiation to get into active region preserving this way all the advantages compared to p-n junction.

Technology and physical properties of $Hg_3In_2Te_6$ single crystals and their analogues

We have synthesized $Hg_3In_2Te_6$ single crystals and their more wide-gap analogues $Hg_2CdInGaTe_6$, $Hg_2MnInGaTe_6$ for Shottky diodes and photodiodes preparation.

Schottky photodiodes based on these wide-gap semiconductors are designed for the detectors of near-infrared, visible and ionizing radiation emission, which do not require additional cooling. The latter is associated with a weak dependence of their photosensitivity on temperature.

Getting of given compositions was carried out by synthesis of binary indium and mercury tellurides in stoichiometric ratio. The analogues were synthesized by replacing the multiple stoichiometric relationships of indium and mercury tellurides by gallium, cadmium and manganese tellurides respectively.

The differential thermal analysis (DTA) was carried out to clarify the melting and crystallization temperatures of these compositions.

From DTA it was found that all three compositions of the $Hg_3In_2Te_6$ crystals and their $Hg_2CdInGaTe_6$, $Hg_2MnInGaTe_6$ analogues melt and crystallize at fixed temperatures congruently. Their crystallization temperatures are T_1 = 715±3 °C, T_2= 760±3 °C, T_3 =775±3 °C, respectively.

All rights reserved. No part of contents of this paper may be reproduced or transmitted in any form or by any means without the written permission of Trans Tech Publications, www.ttp.net. (ID: 194.44.128.2-08/05/15,13:34:32)

Single crystal growing of these compounds was carried out by zone melting in quartz ampoules with simultaneous rotation around their axes in the magnetic fields. This led to the continuous mixing of the melt and to the alignment of the component composition and crystallization front in zone. As a result, uniform distribution of components in the growing crystal has been achieved.

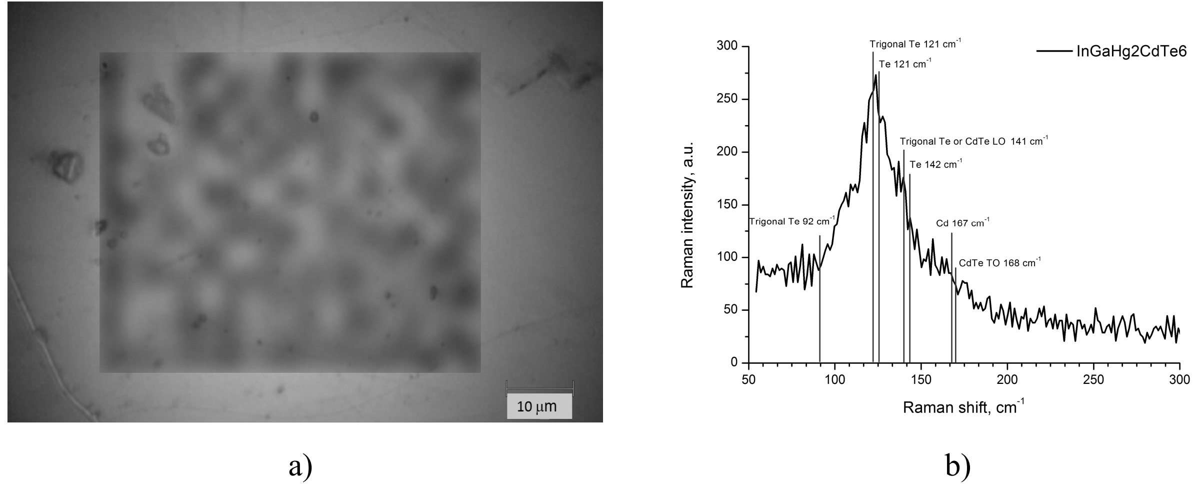

a) b)

Fig. 1. Raman mapping (a) and Raman spectra (b) of $InGaHg_2CdTe_6$.

Te distribution in $InGaHg_2CdTe_6$ was studied by μ-Raman mapping. μ-Raman map indicated inhomogeneous Te distribution, as shown in fig. 1. Inhomogeneity is characterized by 5 μm feature size.

Crystal lattice structure was studied by X-ray Debye-Scherrer method at Fe-K_α radiation with λ = 1.94 Å wavelength using the scheme of backward shooting. The lattice constants were defined (see table 1).

From comparison of d_{hkl} experimental values with calculated, it was determined that the investigated crystals have lattice of sphalerite F43m (B_3) structural type. The nature of the lattice periods decrease for crystals of derivative compounds can be explained by the fact that Hg and In atoms in $Hg_3In_2Te_6$ are partially replaced by Mn, Cd and Ga atoms with a smaller radius.

Table 1 Crystal structure

Material	θ_{hkl}	d_{hkl}, Å	a_{hkl}, Å
$Hg_3In_2Te_6$	65°38’	1,063	6,2912
$Hg_2CdInGaTe_6$	66°07’03”	1,056	6,2529
$Hg_2MnInGaTe_6$	69°53’05”	1,026	6,1032

The corresponding values of band gaps for $Hg_3In_2Te_6$ crystals (E = 0.72 ±0.02 eV), $Hg_2CdInGaTe_6$ (E = 0.95 ±0.02 eV), $Hg_2MnInGaTe_6$ (E = 1.23 ±0.02 eV) at T= 300K were determined by standard optical methods using dependence of the square of the absorption coefficient on the energy of the incident photon at intrinsic absorption edge. As an example, such spectral dependences for $Hg_3In_2Te_6$ crystal at three temperatures is represented in fig.2

Temperature dependences of resistivity (ρ), conductivity (σ) and Hall effect constant (R_x) were measured at all compositions in the range 80-450 K. These measurements revealed that the temperature dependence of the resistivity is described by two activation energies E_1 and E_2 given in Table 2.

Table 2 Electrical characteristics of $Hg_3In_2Te_6$, $Hg_2CdInGaTe_6$ and $Hg_2MnInGaTe_6$ crystals

Crystal	T=295 K			$\lg\rho = f\left(\frac{10^3}{T}\right)$		$\lg\left(R_x T^{3/2}\right) = f\left(\frac{10^3}{T}\right)$
	σ, $(\Omega\cdot cm)^{-1}$	R_x, cm^3/ Coulomb	$\mu_n=\sigma R_x$, $cm^2/V\cdot s$	E_1, eV	E_2, eV	E_D, eV
$Hg_2MnInGaTe_6$	$2\cdot10^{-8}$	$8.7\cdot10^4$	41	0.60	0.19	0.58
$Hg_2CdInGaTe_6$	$6.6\cdot10^{-6}$	$4.6\cdot10^6$	30	0.45	0.12	0.41
$Hg_3In_2Te_6$	$7.4\cdot10^{-4}$	$3.7\cdot10^5$	275	0.35	0.08	0.30

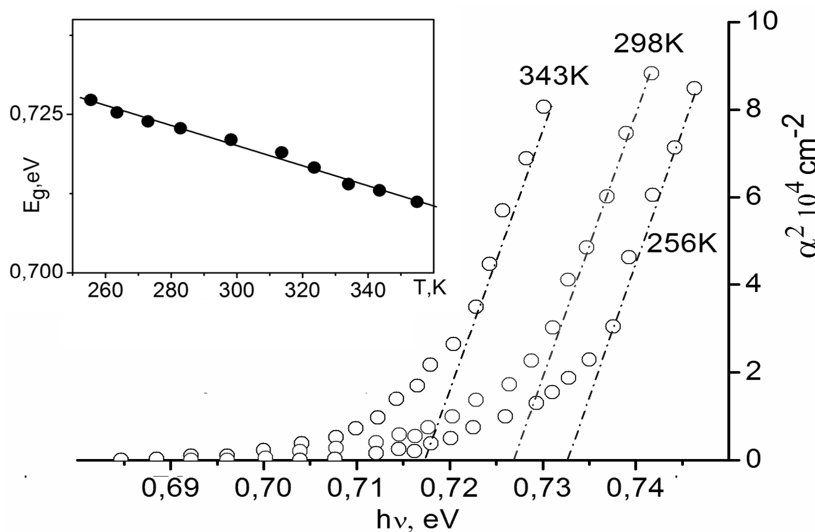

Fig. 2. Absorption curves of the $Hg_3In_2Te_6$ single crystal in the vicinity of $h\nu \approx E_g$ at three temperatures. In the insert, the temperature dependence of the band gap is show.

The activation energy E_1 in the different samples is 0,35-0,60 eV at T>290 K. The activation energy E_2 is determined within 0,19-0,12 eV at T <250 K.

It can be assumed that the activation energy E_1 is connected with ionization of deep compensated donors, which ionization energy E_1=E_D is determined from the temperature dependence of the Hall constant. These deep donors are interstitial indium atoms. Ionization energy E_2 is probably connected with ionization of shallow donors. By analogy with the electrical properties of mercury telluride crystals, where interstitial mercury is a donor, we can assume that the shallow donor is interstitial mercury for the considered solid solutions. Based on these data we can propose a band model structure similar for all compositions of investigated crystals. There were definite values of the band gap widths as $2E_1$ at T=295 K from the comparison of the value of activation energies E_1. From this we can conclude that the energy E_1 corresponds to the energies necessary for the transfer of electrons into the conduction band from the donor level, which in these crystals is placed in the middle of the gap.

Since in the investigated $Hg_3In_2Te_6$ crystals it is impossible to create common p-n junctions through their doping by the impurity elements, we have designed on them the energy structure in the form of Schottky diodes and photodiodes. The last are photosensitive to the optical radiation in the range 0.5-1.6 μm, as well as to the x- and γ- radiation.

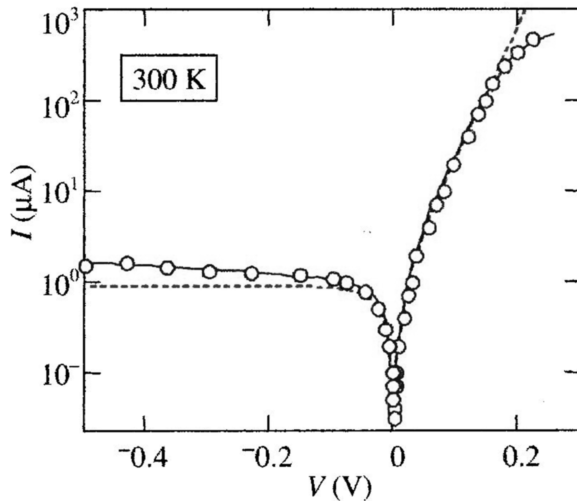

Fig.3. Comparison of I–V characteristics of Ni – $Hg_3In_2Te_6$ diode: measured (circles) and calculated according to the generation-recombination Sah–Noyce–Shockley theory (solid line). The dashed line shows the calculation results according to the thermionic theory.

Transport properties and photoelectric characteristics of the diodes

Schottky diodes were fabricated using vacuum thermal or magnetron sputtering of semi-transparent nickel films of 200 Å thickness or In_2O_3SnO films of 1000 Å thickness on the n-type substrates made of all the investigated crystals. The bottom ohmic contact was manufactured by indium fusing.

Let us consider the charge transport mechanism determining the dark current of the Ni – $Hg_3In_2Te_6$ photodiode, i.e., one of key parameters.

Note that the voltage drop across the series resistance (R_S) of the bulk part of the diode structure takes place at relatively large forward currents. The R_S value can be found from the voltage dependence of the diode differential resistance at forward bias in the saturation range. The I–V characteristic of Ni – $Hg_3In_2Te_6$ (S=1.3 mm^2) diode, plotted in semi-logarithmic scale taking into the account the voltage drop across the resistance R_S, is shown in Fig. 3. As it is seen, the portion of the forward I–V characteristic, where the current is proportional to exp(qV/kT)-1, is clearly observed. The results presented below show that the I–V characteristic of the Ni - $Hg_2In_3Te_6$ diode is determined by the generation-recombination processes.

According to the Sah–Noyce–Shockley theory the current caused by generation-recombination in the space-charge region of the diode is expressed as [3]:

$$I_{g-r} = Aq\int_0^W \frac{n(x,V)p(x,V)-n_i^2}{\tau_{p0}[n(x,V)+n_1]+\tau_{n0}[p(x,V)+p_1]}dx\,, \tag{1}$$

where A is the area of the junction, n(x, V) and p(x, V) are the carrier concentrations in the corresponding bands, τ_{n0}, τ_{p0} are the effective lifetimes of electrons and holes in the space-charge region.

The values of n_1 and p_1 are the equilibrium concentrations of electrons and holes, respectively, under the condition that the Fermi level coincides with the considered level, i.e., $n_1 = N_c \exp[-E_t/kT]$ and $p_1 = N_v \exp[-(E_g - E_t)/kT]$. Here $N_c = 2(m_n kT/2\pi\hbar^2)^{3/2}$ and $N_v = 2(m_p kT/2\pi\hbar^2)^{3/2}$ are the effective state densities in the conduction and valence bands, respectively, (m_n=0,47m_0, m_p=0,35m_0 are the effective masses of electrons and holes, respectively), E_t is the energy spacing between the generation-recombination energy level and the bottom of the conduction band.

Counting off the energy from the bottom of the conduction band in the bulk of the diode structure and the coordinate *x* from the semiconductor surface, one can write for the concentrations of electron and holes in a point x at a voltage *V*:

$$n(x,V) = N_c \exp\left[-\frac{\Delta\mu + \varphi(x,V)}{kT}\right], \tag{2}$$

$$p(x,V) = N_v \exp\left[-\frac{E_g - \Delta\mu + \varphi(x,V) - qV}{kT}\right], \tag{3}$$

where φ(*x,V*) is the potential energy of the electron in the space-charge region, Δμ - distance Fermy level from conductivity band bottom

$$\varphi(x,V) = (\varphi_0 - qV)\left(1 - \frac{x}{W}\right)^2, \tag{4}$$

and W is the width of space-charge region:

$$W = \sqrt{\frac{2\varepsilon\varepsilon_0(\varphi_0 - qV)}{q^2(N_d - N_a)}}. \tag{5}$$

In Eq. (5) ε_0 is the electrical constant, ε is the dielectric constant of the semiconductor, $\varphi_0=qV_{bi}$ is the barrier height at the semiconductor side and N_d-N_a is the uncompensated donor concentration.

The solid line in Fig. 3 results from calculations of I–V characteristic described by Eq. (1) using Eqs. (2) – (5). In the computation, the carrier lifetime, found from the decay curve of photocurrent, was taken equal to $\tau = \tau_{n0} = \tau_{p0} = 3\cdot10^{-8}$ s, while for fitting the calculation results with the measured data the concentration of uncompensated donors was taken equal to N_d-N_a=$2.5\cdot10^{13}$ cm^{-3}. It follows from the Sah–Noyce–Shockley theory at conditions providing the generation-recombination level to be near the middle of the bandgap, that the forward current follows the dependence I~exp(qV/nkT)-1 with n close to 2. If the generation-recombination level is remarkably far from the middle of the band gap, the forward current follows the dependence I~exp(qV/nkT)-1 with n ≈ 1 at low bias voltages, and only at higher voltages such dependence transforms into I~exp(qV/nkT)-1 with n ≈ 2. The voltage, at which one dependence transforms into another, is determined by the ionization energy of the generation-recombination centers E_t and the barrier height φ_0. The energy E_t also affects the rectification coefficient of the diode.

By varying E_t and φ_0, it is easy to find their values, at which theory best describes the experimental I–V characteristic. The computed results for E_t = 0.236 eV and φ_0 = 0.39 eV are shown in Fig. 3. As seen, the experimental I–V characteristic of the Ni – $Hg_3In_2Te_6$ photodiode both at forward and reverse biases very well correlates with the Sah–Noyce–Shockley theory.

The spectral responsivity of the Ni-$Hg_3In_2Te_6$ photodiode (in A/W) at room temperature is shown in Fig. 4, a. The spectral characteristics of the samples were recorded using the photoresponse system

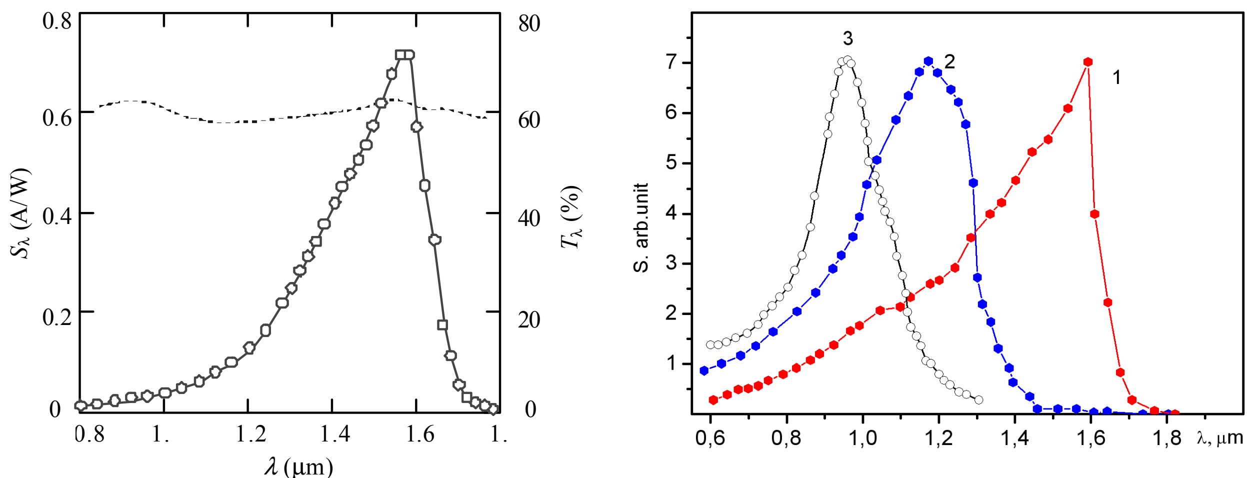

a) **b)**

Fig. 4, a) Responsivity spectrum of a Ni- $Hg_3In_2Te_6$ photodiode. The dashed line shows the optical transmittance of the Ni film on the CdTe substrate; **b)** The relative current monochromatic sensitivity of the photodiode based on $Hg_3In_2Te_6$ (1), $Hg_2CdInGaTe_6$ (2) and $Hg_2MnInGaTe_6$ (3) for comparison.

with a quartz halogen lamp as light source. The spectral distribution of the photon flux at the outlet slit of the system was determined using a calibrated Si photodiode. As seen from this figure, the responsivity maximum is exactly at the wavelength 1.55 μm, i.e., the bandgap and the absorption spectrum of $Hg_3In_2Te_6$ provide the most effective use of $Hg_3In_2Te_6$-based photodiodes for silica-based fiber optic communication systems with the lowest losses. The value of current responsivity in the maximum of the curve is somewhat above 0.7 A/W which is quite close to the responsivity of commercial Ge photodiodes based on p-n junctions.

By dashed line in Fig. 4, a the spectral dependence of transmittance T of the Ni film evaporated on the CdTe wafer is also shown. The choice of CdTe is motivated by its optical transparency in the $\lambda >$ 0.85 μm range and its refraction coefficient, which is not very different from that of $Hg_3In_2Te_6$. Finally, the efficiency of the Ni-$Hg_3In_2Te_6$ photodiode can be increased by an antireflection coating.

The currently achieved responsivity of 0.7 A/W corresponds to the quantum efficiency 0.56 electron/photon ($h\nu$ = 0.8 eV for λ = 1.55 μm). The internal efficiency of a Schottky diode is determined by the expression [4]:

$$\eta = \frac{1+\dfrac{S}{D_{\mathrm{p}}}\left(\alpha+\dfrac{2}{W}\dfrac{\varphi_{\mathrm{o}}-qV}{kT}\right)^{-1}}{1+\dfrac{S}{D_{\mathrm{p}}}\left(\dfrac{2}{W}\dfrac{\varphi_{\mathrm{o}}-qV}{kT}\right)^{-1}}-\frac{\exp(-\alpha W)}{1+\alpha L_{\mathrm{p}}}, \tag{6}$$

where S is the surface recombination velocity, α is the absorption coefficient, D_p and L_p are the diffusion coefficient and diffusion length of minority carriers (holes), respectively.

The above-mentioned values of φ_o and $N_d - N_a$ will be used for η calculations using Eq. (6) at V = 0 and ε = 10. We will assume that the hole mobility in $Hg_3In_2Te_6$ is one order of magnitude lower than that of the electrons, so their diffusion coefficient at room temperature is 0.25 $cm^2/(V{\cdot}s)$ The absorption coefficient at the wavelength 1.55 μm is 5000 cm^{-1} [5], so according to the Eq. (6), the internal efficiency of the photodiode at this wavelength is 0.85, and the responsivity is 1.063 A/W. Comparison of the calculated quantum efficiency 0.85 with the measured value of 0.56 shows that the coefficient for the radiation transmission into the photodiode active region is 0.64, i.e. close to the measured transmittance of the Ni layer (the dashed line in Fig. 4, a).

If $N_d - N_a$ decreases, the space-charge region widens and larger portion of radiation is absorbed in it. However, the electric field in the space-charge region weakens and the effect of surface recombination enhances. Competition of these factors leads to the existence of an optimal value for $N_d - N_a$, at which the responsivity is maximal. By varying $N_d - N_a$ in Eq. (6), it is easy to verify that a maximum values of quantum efficiency and responsivity are 0.879 and 1.098 A/W, respectively, at $N_d - N_a = 1{\times}10^{13}$ cm^{-3}[6].

Thus, the responsivity of Ni-$Hg_3In_2Te_6$ photodiode is higher than the state of the art one for Ge photodiodes. This is understandable, since in $Hg_3In_2Te_6$, the wavelength of 1.55 μm corresponds to the energy of the direct interband transitions, whereas in Ge of indirect ones (the absorption coefficient in Ge at the same wavelength is 460 cm^{-1}). As temperature increases from –20 °C to +50 °C the photoresponse of the Ge photodiode reduces almost by 2 orders of magnitude, whereas for the $Hg_3In_2Te_6$ photodiode – only in 2.5-3 times [6].

The relative current monochromatic sensitivity of Schottky diodes based on $Hg_2CdInGaTe_6$ and $Hg_2MnInGaTe_6$ is similar to those in the $Hg_3In_2Te_6$ (see Fig.4, b). The maxima of the spectral dependence of photodiodes on the $Hg_3In_2Te_6$, $Hg_2CdInGaTe_6$ and $Hg_2MnInGaTe_6$ substrates are at the wavelength λ_1 =1,55 ±0,05 μm, λ_2=1,17 ± 0.05 μm and λ_3 = 0.95 ± 0.05 μm, respectively. This data is within the error of experiments and are in good agreement with band gap data for these crystals obtained in optical and electrical studies.

These experimental studies and calculations were performed also on Schottky diodes with the In_2O_3:SnO top coating.

Under irradiation of $Hg_3In_2Te_6$-based Schottky photodiodes by X-rays it was found that the dependence of the signal increment with dose increase of X-ray radiation has the form $I_R \sim R^{0.5}$, where “R” mean X-ray dosage. Dose range was 10 $mRs^{-1} \div 50$ Rs^{-1}. Roentgen sensitivity was defined as the ratio of the increment of the photocurrent to the dose and to the voltage applied to the diode. This value was 0.1 $mAV^{-1}R$ at a dose 10 mRs^{-1}.

Such a dependence of the photocurrent increase was observed upon irradiation of $Hg_3In_2Te_6$-based Schottky photodiodes by γ-radiation. MPX-γ-Co installation with photon energies 1.2 MeV and dose rate 60 R/s was used for irradiation. Measurements were carried out within the power of 10^{-2} R/s to 60 R/s. Devices made from $Hg_3In_2Te_6$ crystals have high X-ray and gamma-ray sensitivity in comparison with other materials that are used for the manufacture of similar detectors. There is a single species of signal photocurrent dependence on the dose in a wide range of radiation dose changing.

It was shown that the possibility exists to improve homogeneity of the InGaN by laser radiation [7]. This method will be used for improvement of the homogeneity of $Hg_3In_2Te_6$-based crystals too.

Summary

The methods of synthesis and growth of $Hg_3In_2Te_6$, $Hg_2CdInGaTe_6$ and $Hg_2MnInGaTe_6$ crystals stable to high-level radiation are developed. Their structural, electrical and optical properties were studied. On their basis Schottky photodiodes have been fabricated which are photosensitive to the optical radiation within 0.4-1.6 μm range and to the X-ray and γ-radiation. Their photoelectric and transport properties are investigated.

Accounting for high radiation stability of $Hg_3In_2Te_6$ and its analogues the creation of infrared, visible and hard radiation detectors on their basis, which are stable in a wide range of doses and energies, seems to be very perspective.

Acknowledgments

This research has been supported by the European Social Fund within the project “Elaboration of Innovative Functional Materials and Nanomaterials for Application in Environment Control Tehchnologies” 1DP/1.1.1.2.0/13/APIA/VIAA/30.

References

[1] V. M. Koshkin, I.N. Volovichev, Yu.G. Gurevich, L.P. Gal’chinetskiy, I.M. Rarenko, Materials and devices with giant radiation resources, Kharkov, 2006.

[2] V.M. Koshkin, Yu. Dmitriev, Chemistry and Physics of Compounds with Loose Crystal Structure, Harwood Acad. Publishers. Ser. Chemical Reviews, England – Switzerland, 1994.

[3] C. Sah, R. Noyce, and W. Shokley, Carrier Generation and Recombination in P-N Junctions and P-N Junction Characteristics, Proc. IRE 45, 1228 (1957).

[4] M. Lavagna, J.P. Pique, and Y. Marfaing, Theoretical analysis of the quantum photoelectric yield in Schottky diodes, Solid State Electronics 20 (1977) 235-240.

[5] L.A. Kosyachenko, I.I. German, S.Yu. Paranchych, and S.G. Guminetsky, Optical Characteristics of $Hg_3In_2Te_6$ as a Material for 1.55-μm Photodiodes, Ukr. J. Phys. 51, (2006) 1048-1053.

[6] L.A. Kosyachenko, I.S. Kabanova, V.M. Sklyarchuk, O.F. Sklyarchuk, I.M. Rarenko, Phys. St. Sol. A206 (2009) 351-355.

[7] G. Tamulaitis, D. Dobrovolskas, J. Mickevičius, V. Kazlauskiene, J. Miškinis, E. Kuokštis, P. Onufrijevs, A. Medvids, J.-J.Huang, C.-Y.Chen, C.-H.Liao and C.C.Yang, Suppression of defect-related luminescence in laserannealed InGaN epilayers, Phys.Status Solidi C 9 (2012) 1021-1023.